Dynamic Range Enlargement in CMOS Imagers with Buried Photodiode

Vladimir Berezin, Ilia Ovsiannikov, Dmitri Jerdev, Richard Tsai

Micron Imaging, Micron Technology, Inc.
135 N. Los Robles Ave, Pasadena CA, 91101
vberezin@micron.com

Abstract

There are more and more applications that require high dynamic range (hi-dy) for both consume and industrial markets. This paper presents the analysis and experiment results of dynamic range enlargement approach for three to five-transistor (3-5T) pixels with buried photodiode for CMOS image sensors. The improved dynamic range could reach 128dB through the described method by using only 2 knees.

I. Introduction

With recent advancements, CMOS image sensors have become a mature technology, fully competitive with well-established CCDs. Various techniques have been implemented to improve performance of CMOS imagers in the low-light part of the dynamic region. However, high-light handling capability is still a very important feature for consumer products, as well as for many other applications like automotive, machine vision, and security applications, etc.

Many different types of approaches to intrascene dynamic range extension have been described in the literature, but we are focusing only on imagers having both a multiple-knee light transfer curve and well capacity adjustment. The first description of this method can be found in US Patent 3,953,733 by P. Levine of RCA [1]. To obtain enlarged dynamic range on CCD gates the gate voltage was increased in discrete steps. S.Decker et al. presented at ISSCC'98 a similar approach for CMOS imagers [2]. Now, many people are working in this direction [3-5].

This paper presents an old-fashioned technique for dynamic range enlargement in modern CMOS image sensors with buried photodiodes. This approach was initially considered for 3T CMOS imagers long time ago, but has been recently implemented at Micron Imaging for sensors with a buried photodiode. We use variable, from high to low, amplitude saturation control pulses during integration time to obtain an appropriate light transfer function to increase intrascene dynamic range. The additional control pulses (pointers) with variable amplitude determine a desirable number of knees and make sensor implementation easy and flexible.

II. Sensor Operation

Higher dynamic range in 3T pixels is achieved by introducing an extra pixel reset operation to selectively remove photo-charge and restart integration (see Fig. 1a). V_{RST} of the extra reset is set to a lower-than-normal value. This causes pixels with exposure higher than a threshold to be soft-reset to approximately $V_{RST} - V_{TH}$, where V_{TH} is the reset transistor threshold voltage. It is assumed that the scene illumination is constant. This approach was extended to 4T (Fig. 2a) and 5T (Fig. 1b) structures. For 4T, saturation control signal is applied to TX instead of reset gate. For 5T, this signal is applied to AB gate.

A threshold exposure divides the operating range into the normal and hi-dy parts. The level of intermediate saturation control pulses sets the magnitude of the inflexion points. The slope of the transfer curve in the hi-dy diapason is always lower than in the normal, by a factor of T_2 / T_{INT}, where T_{INT} is the total integration time and T_2 is the "lead" time of the second, intermediate saturation control pointer.

Diagrams describing the operation of 4T pixel in hi-dy mode are shown in Fig. 3. Fig. 3a shows charge accumulation in the pixel as a function of integration time for several different illumination intensities. Each knee has a maximum charge value that it can handle determined by the saturation control signal. If intensity of illumination is less than value required to saturate the given knee, the charge accumulation trend does not change at the point of intermediate transfer pulse. Otherwise the value of charge is brought to the maximum level for given knee by this pulse. Example of position and relative amplitudes of the intermediate reset

pulses is shown in Fig. 3b. Fig. 3c shows the pixel output signal as a function of illumination. The fact that each following knee starting from the first to the last has less slope than previous means that it can handle more intensive light thus resulting in extended dynamic range.

III. Operation and Improvement Analysis

In order to analyze operation of the 4T pixel in hi-dy mode let introduce the following definitions: **n** – number of knees implemented in the light transfer curve; I_{SAT} – maximum illuminance value that can be detected in the pixel; α_i – i-th breakpoint illuminance normalized to I_{SAT}; V_{SAT} – maximum signal value that can be detected in the pixel; β_i – part of the signal range assigned for the given i-th knee; T_{INT} – total integration time; τ_i – part of the total integration time assigned for the given i-th knee; S – pixel sensitivity, which is the same for all knees.

Based on these definitions: $\alpha_i = I_i / I_{SAT}$ where I_i – breakpoint illuminance level for i-th knee; $\beta_i = \Delta V_i / V_{SAT}$ where ΔV_i – pixel output signal discrete for i-th knee; $\tau_i = \Delta T_i / T_{INT}$ where ΔT_i – integration time discrete for i-th knee; $\alpha_n = 1$; $\Sigma\beta_i = 1$; $\Sigma\tau_i = 1$

Now we can determine the pixel output signal discrete for each knee:

$$\Delta V_i = I_i * \Delta T_i * S = \alpha_i * \tau_i * I_{SAT} * T_{INT} * S$$

According to the definition:

$$\beta_i = \Delta V_i / V_{SAT} = \alpha_i * \tau_i * I_{SAT} * T_{INT} * S / V_{SAT} = \alpha_i * \tau_i * K$$

where K is determined by pixel design (S and V_{SAT}) and operation conditions (I_{SAT} and T_{INT}), and is the same for all knees

$$K = I_{SAT} * T_{INT} * S / V_{SAT} = \beta_i / (\alpha_i * \tau_i)$$

If $\Sigma\tau_i = \Sigma (\beta_i/\alpha_i)/K = 1$ $\quad K = \Sigma (\beta_i / \alpha_i)$

If for the last knee (i = n) $\alpha_n = 1$ $\quad K = \beta_n / \tau_n$.

We can determine saturation illuminance based on the definition of the coefficient K

$$I_{SAT} = K * V_{SAT} / (T_{INT} * S)$$

Saturation signal for pixel standard operation (without knee) could be written as

$$I_{REF} = V_{SAT} / (T_{INT} * S)$$

The smallest detectable signal is equal to the pixel noise and does not change for multi-knee mode in comparison with standard mode. So dynamic range is increased by a factor of

$$DRF = I_{SAT} / I_{REF} = K$$

For reference operation mode (no knees) $n = 1$, $\beta_n = 1$; $\tau_n = 1$ and $K = \beta_n / \tau_n = 1$. There is no dynamic range improvement without knees.

If integration time for the last knee is equal to row time (for NTSC - $\tau_n = 1/525$), dynamic range extension is determined as:

$\beta_n = 0.2$	K = 100 (40dB)
$\beta_n = 0.3$	K = 157 (44dB)
$\beta_n = 0.4$	K = 210 (46.4dB)
$\beta_n = 0.5$	K = 262 (48.4dB)
$\beta_n = 0.6$	K = 315 (50dB)

Using these simple equations, we can determine **K** and τ_i for given α_i and β_i, which fully describe required light transfer curve. For the given light transfer curve with three knees (Fig. 3b):

$\alpha_1 = 0.33$	$\beta_1 = 0.6$
$\alpha_2 = 0.66$	$\beta_2 = 0.3$
$\alpha_3 = 1$	$\beta_3 = 0.1$

$$K = \Sigma (\beta_i / \alpha_i) = 0.6/0.33+0.3/0.66 +0.1/1 = 2.355$$

$$\tau_1 = \beta_1 / (\alpha_1 * K) = 0.6/(0.33*2.355) = 0.764\ (76\%)$$
$$\tau_2 = \beta_2 / (\alpha_2 * K) = 0.3/(0.66*2.355) = 0.193\ (20\%)$$
$$\tau_3 = \beta_3 / (\alpha_3 * K) = 0.1/(1.00*2.355) = 0.043\ (4\%)$$

IV. Experimental Results

There are two sets of measurements that were performed. In the first set (Fig. 4,d-f) we changed the position of the intermediate reset while changing its amplitude. In the second one (Fig. 4,a-c) we kept the position of the intermediate reset pulse constant while changing its amplitude.

In the first series of measurements, we positioned the intermediate reset pulse at 1/8 of the total integration time before the end of integration cycle. The amplitude of this pulse varied in the range 0-3.0 V. At a value of the intermediate reset pulse equal to 0 working mode of the sensor was the same as normally used as no knees in the response were observed (Fig. 4a). If this reset level was increased to 2.0V the knee in the response starts to appear. The response curve separates into two clearly identifiable regions with higher and lower sensitivity. The

fist part before the knee coincides with the response of the normal pixel, as one would expect. The second part, less sensitive region, is the one for which the effective integration time was only 1/4 of the total integration period. The sensitivity decrease for this region was about the same. If we further change the reset level the position of the knee shifts accordingly. Higher reset levels assign larger part of the useful voltage swing of the sensor for region with lower sensitivity thus moving knee point closer to the zero signal value. Parts of the response curves belonging to low sensitivity are virtually parallel independently on the knee position. This is also expected. If the intermediate reset level is equal to the level of the pixel reset the region with high sensitivity must disappear. We did not reach that point but this trend is obvious in the graph.

Behavior of the temporal noise is shown in Fig. 4 (b, e). To understand it we have to account for two processes of noise generation (apart from readout noise). First process is obviously shot noise and results from photon detection. This source of noise grows as SQR (N). The second source of noise is consequence of intermediate reset itself and it only appears for those pixels, which were subjected to the intermediate reset, i.e. such pixels where all the accumulated charge above the reset has been discarded. These pixels are effectively reset and thus noise floor for such pixels becomes equal to that for the soft reset, which is around kTC/2. This point where reduction of the noise occurs is well defined for all reset levels except zero. This noise source cannot be removed by CDS in the 4T pixel as it only cancels kTC noise for floating diffusion. Charge, which is still preserved in the pixel after reset procedure, determines the position of the knee on the response curve when it is readout to the floating diffusion. The rest of the period when pixel is exposed to light additional charge is introduced and the corresponding noise is added. Overall noise becomes SQR ($kTC/2+N_e^2$). The Fig. 4 shows temporal nose for the second mode of operation and is similar. The conclusion here is that there is no additional noise source associated with hi-dy operation when pixel is operating in the small signal region and there is additional kTC noise, which is added after passing knee point. Since normally this point will be at some significant signal level this noise source should not be noticeable.

Fig. 4(c,f) show behavior of signal non-uniformity during two mentioned modes of operation. There is significant additional FPN added to the signal after it passes knee point. The origin of this increase is the variation in Vth for transfer gate transistors.

Conclusion

We have successfully obtained light transfer curves with two linear regions corresponding to high and low device sensitivity for 3T and 4T Buried PD structures, see Fig. 5 and 6. Sensor dynamic range was significantly increased. A realistic, non-aggressive improvement in dynamic range for the VGA, 30 FPS double-knees operation sensors is 48dB. Considerably larger numbers and optimal shape of light transfer curve can be obtained using additional knee points. Recent developments in CMOS imagers have yielded an 80dB dynamic range. Combined with the 48dB range extension achieved through the described method, we can realistically achieve a 128dB pixel operation using just double knees.

Acknowledgments

These experimental results were made possible by the effort of many Micron Technology team members from both Boise and Pasadena. Their contributions are greatly appreciated.

References

[1] P. A. Levine "Method of Operating Imagers", US Patent 3,953,733, Apr.27, 1976.
[2] S. J. Decker, R. D. McGrath, K. Brehmer, and C. G. Sodini, A 256x256 CMOS imaging array with wide dynamic range pixels and column-parallel digital output." IEEE J. of Solid State Circuits, Vol.33, pp.2081-2091, Dec. 1998.
[3] S. T. Smith, P. Zalud, J. Kalinowski, N. J. McCaffrey, P. A. Levine, M. L. Lin, Sarnoff Corp "BLINC: a 640x480 CMOS active pixel video camera with adaptive digital processing, extended optical dynamic range, and miniature form factor", SPIE Electronic Imaging, San Jose, CA, January 2001.
[4] A. El Gamal, High Dynamic Range Image Sensors, Tutorial at ISSCC, San Francisco, CA, February 2002.
[5] H.Witters, T.Walschap, G. Vanstraelen, G.Chapinal, G.Meynants, B.Dierickx, "1024 x 1280 Pixel Dual Shutter APS for Industrial Vision", SPIE Electronic Imaging, Santa Clara, CA, January 2003.

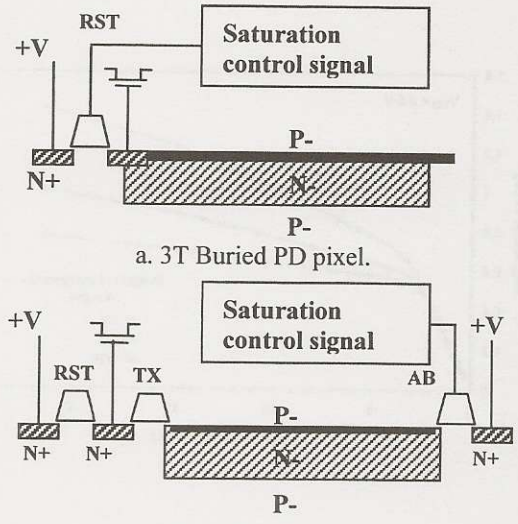

Fig. 1. Dynamic range enlargement for different kind of CMOS imagers.

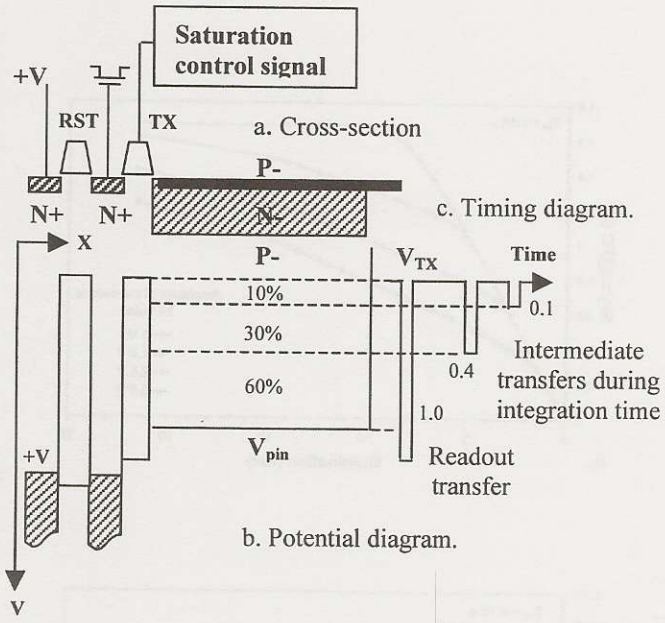

Fig. 2. Dynamic range enlargement for 4T Buried PD imagers.

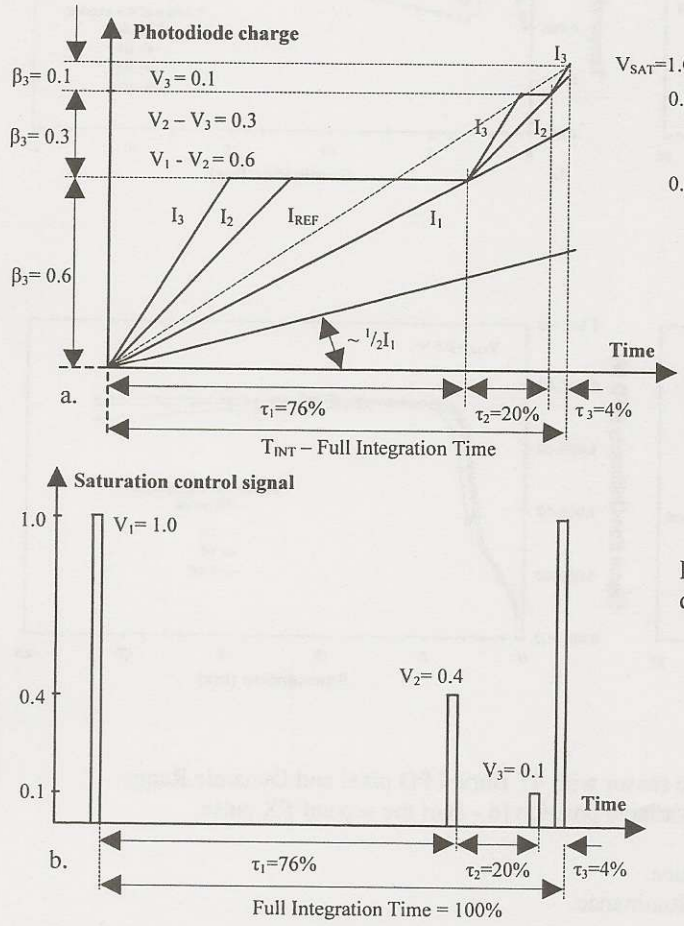

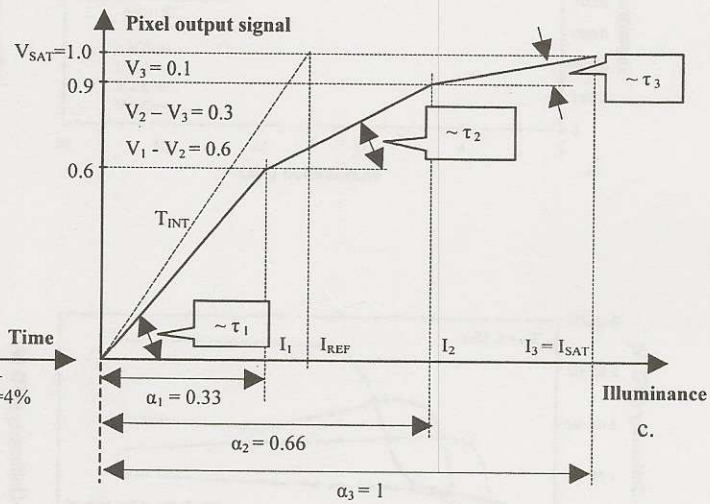

Fig. 3. Graphical representation of pixel operation with dynamic range enlargement based on multi-knee approach.

a. Photodiode charge vs. time for variable illuminance.
b. Multiple saturation control pulses with variable high level.
c. Multi-knee light transfer function.

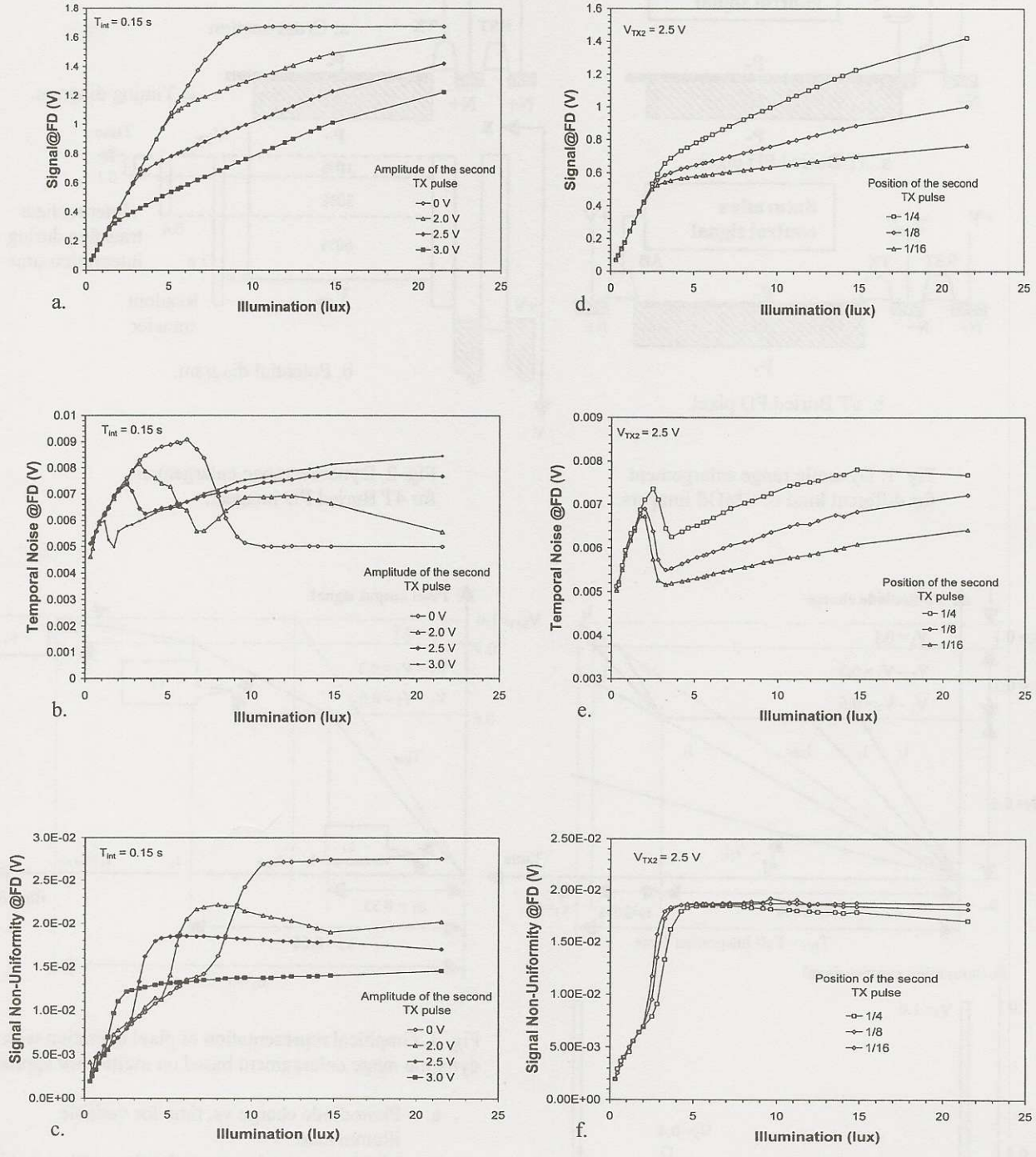

Fig. 4. Characterization results of CMOS image sensor with 4T Buried PD pixel and Dynamic Range enlargement for variable amplitude (a - c) and variable position (d - f) of the second TX pulse.

a, d Light transfer curves.

b, e Temporal Noise vs. Illuminance.

c, f Signal Non-Uniformity vs. Illuminance.

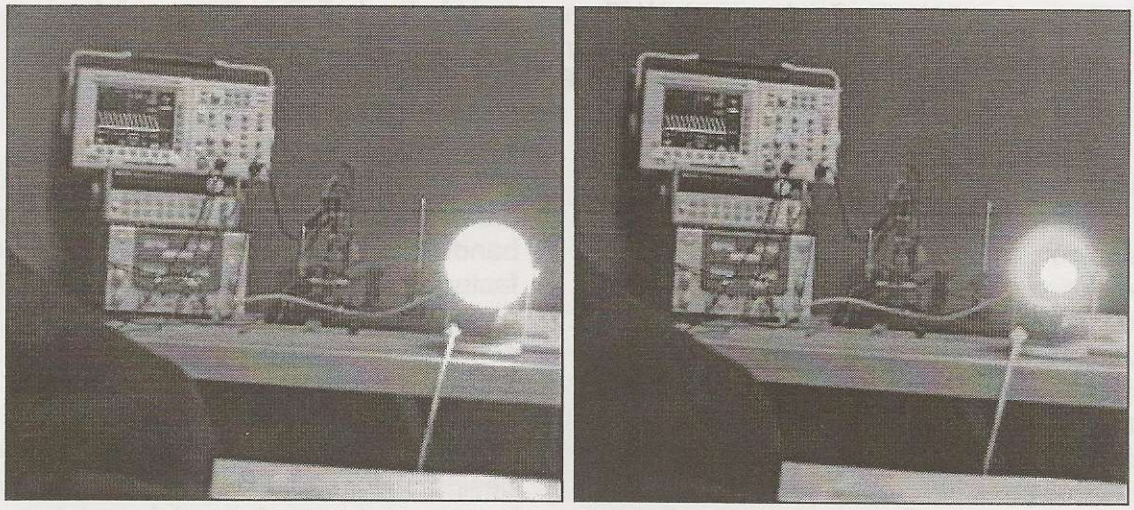

Fig.5. Lamp interior becomes visible in 3T CMOS imagers with buried PD and intermediate resets.

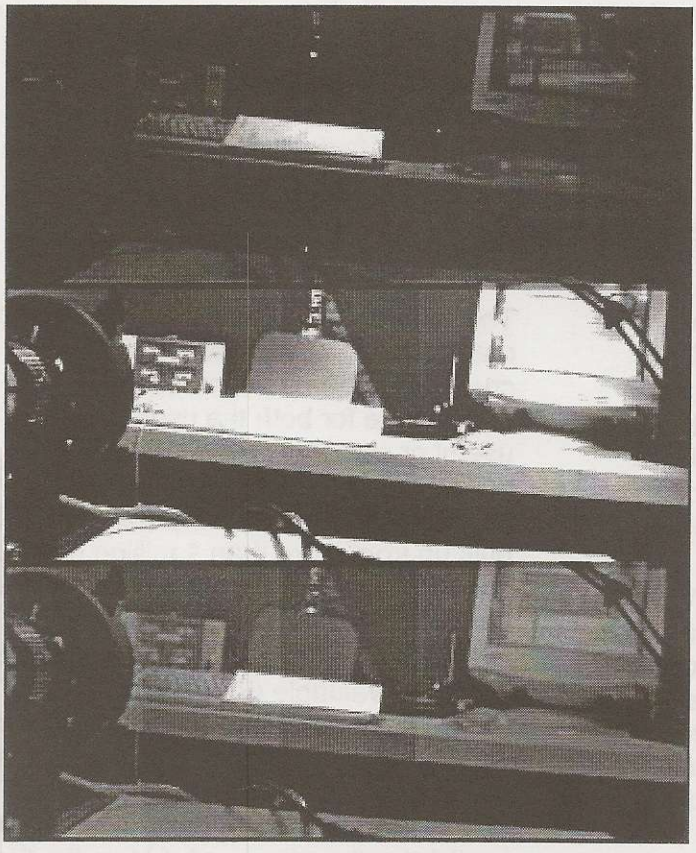

Fig.6. Illustrations of dynamic range extension in 4T CMOS imagers with Buried PD and intermediate transfer (TX) pulses.